Spin-to-Orbital Optical Angular Momentum Conversion in Liquid Crystal "q-Plates": Classical and Quantum Applications

Article *in* Molecular Crystals and Liquid Crystals · June 2012

DOI: 10.1080/15421406.2012.686710

CITATIONS
32

READS
1,364

7 authors, including:

Ebrahim Karimi
University of Ottawa
329 PUBLICATIONS **13,015** CITATIONS

SEE PROFILE

Bruno Piccirillo
University of Naples Federico II
104 PUBLICATIONS **5,116** CITATIONS

SEE PROFILE

Enrico Santamato
University of Naples Federico II
153 PUBLICATIONS **6,681** CITATIONS

SEE PROFILE

Mol. Cryst. Liq. Cryst., Vol. 561: pp. 48–56, 2012

ISSN: 1542-1406 print/1563-5287 online
DOI: 10.1080/15421406.2012.686710

Taylor & Francis
Taylor & Francis Group

Spin-to-Orbital Optical Angular Momentum Conversion in Liquid Crystal "q-Plates": Classical and Quantum Applications

L. MARRUCCI,[1,2,*] E. KARIMI,[1] S. SLUSSARENKO,[1]
B. PICCIRILLO,[1] E. SANTAMATO,[1] E. NAGALI,[3]
AND F. SCIARRINO[3]

[1]Dipartimento di Scienze Fisiche, Università di Napoli "Federico II", Complesso di Monte S. Angelo, via Cintia, 80126 Napoli, Italy
[2]CNR-SPIN, Complesso di Monte S. Angelo, via Cintia, 80126 Napoli, Italy
[3]Dipartimento di Fisica dell'Università di Roma "La Sapienza", Roma 00185, Italy

The angular momentum of light can be split into a spin and an orbital component (SAM and OAM). A few years ago, an optical process involving a conversion of angular momentum from one form to the other was conceived and experimentally demonstrated in a singular patterned liquid crystal cell, also known as "q-plate". In this paper, after reviewing the q-plate concept and technology, we will survey some of the most significant results that have originated from it, with particular attention to the possibility of realizing a physical one-to-one mapping between the polarization Poincaré sphere and an OAM subspace of an optical beam or of a single photon.

Keywords Liquid crystals; orbital angular momentum; quantum information

I. Introduction

Besides energy and linear momentum, one can associate to the electromagnetic field also an angular momentum (AM) content. In the paraxial limit, e.g. when dealing with a beam-like optical field, this AM can be naturally split into two components: (i) a spin-like AM component (SAM), associated with the ellipticity of the light polarization, and (ii) an orbital AM component (OAM), associated with a nonzero average azimuthal gradient of the field, as in the case of a helical wavefront. While polarization and SAM have been widely studied and utilized in the photonics technology since a long time, the interest in OAM is more recent, and it has become very intense only in the last twenty years (see, e.g., Refs. [1, 2] and references therein).

Liquid crystals (LC) are materials that are particularly well suited for interacting with the angular momentum of light, owing to their anisotropic properties, to their softness allowing for a relatively easy spatial patterning, and to the their flexibility to an external control by means of electromagnetic fields [3]. The LC optical response shows a great sensitivity to the specific interaction geometry, and the LC nonlinear optical properties

*Address correspondence to L. Marrucci. Tel: +39-081-676124. E-mail: lorenzo.marrucci@na.infn.it

can be also largely modified by altering only slightly the material composition, e.g. by adding suitable dopants (see, e.g., Refs. [4–10] and references therein). Being birefringent, LCs couple very naturally with the SAM component of light, but more recently it has been shown that they can be also used to control effectively the OAM component. More precisely, a LC cell with a singular pattern of the nematic director can introduce a strong spin-orbit coupling in the light propagation, resulting into strong variations of both SAM and OAM. In particular geometries, these variations can be interpreted as a spin-to-orbital conversion of the angular momentum of light [11]. This is the physical principle behind the so-called "q-plate" [11–13], a LC-based device that has been attracting increasing attention in the last years, owing to its possible applications in both classical and quantum photonics [14]. Many of these applications descend from the possibility of establishing a physical "one-to-one mapping" between the polarization Poincaré sphere and an isomorphic OAM subspace of an optical beam or of a single photon.

This paper is structured as follows. In Section II, we review the q-plate concept and recent technology. Next, in Section III, we will discuss the mapping between polarization and OAM spaces that can be realized by means of the q-plate technology. Finally, in Section IV, we will briefly survey the recent results obtained in quantum photonics, based on this mapping, and summarize our conclusions.

II. The q-Plate: Concept and Technology

A q-plate is built as a planar LC cell having thickness and birefringence selected so as to induce a homogeneous birefringent phase retardation δ at the working wavelength λ, for light propagation perpendicular to the cell plane walls (z axis). The LC nematic director $\mathbf{n}$ is assumed to be uniform in the z direction, but inhomogeneous in the xy plane of the cell, according to a prescribed pattern $\mathbf{n}(x, y) = \mathbf{n}(r, \varphi)$, where r and φ are the polar coordinates in the xy plane. In particular, the q-plate pattern is specified by the following expression:

$$\alpha(r, \varphi) = \alpha_0 + q\varphi \tag{1}$$

where $\alpha(r,\varphi)$ is the angle between the director $\mathbf{n}(x, y)$ and the x axis, α_0 is a constant angle specifying the director "initial" orientation on the axis x, and q is an integer or semi-integer constant specifying the q-plate *topological charge*.

It can be easily proved that the Jones matrix $\mathbf{M}$ describing the q-plate action on the optical field at each transverse position r,φ is the following:

$$\mathbf{M}(r, \varphi) = \cos\frac{\delta}{2}\begin{bmatrix} 1 & 0 \\ 0 & 1 \end{bmatrix} + i \sin\frac{\delta}{2}\begin{bmatrix} \cos 2(\alpha_0 + q\varphi) & \sin 2(\alpha_0 + q\varphi) \\ \sin 2(\alpha_0 + q\varphi) & -\cos 2(\alpha_0 + q\varphi) \end{bmatrix} \tag{2}$$

where δ is the above-mentioned birefringent phase retardation.

Let us now assume that at the q-plate input there is circularly polarized wave (with SAM $= \pm\hbar$) having an arbitrary OAM given by $m\hbar$, where m is the OAM quantum number. Its Jones electric-field vector is then given by

$$\mathbf{E}_{in}(r, \varphi) = E_0(r)\begin{bmatrix} 1 \\ \pm i \end{bmatrix} e^{im\varphi} \tag{3}$$

where $E_0(r)$ is a radially-dependent arbitrary amplitude and $\pm$ is $+$ for the left-circular case and $-$ for the right-circular one. At the q-plate output, we then obtain the following

field:

$$\mathbf{E}_{out}(r,\varphi) = E_0(r)\cos\frac{\delta}{2}\begin{bmatrix}1\\ \pm i\end{bmatrix}e^{im\varphi} + i\,E_0(r)\sin\frac{\delta}{2}e^{\pm i2\alpha_0}\begin{bmatrix}1\\ \mp i\end{bmatrix}e^{im'\varphi} \tag{4}$$

where

$$m' = m \pm 2q. \tag{5}$$

This output field can be interpreted as a *coherent superposition* of a first wave that has the same circular polarization and OAM as the input one, and a second wave having reversed circular polarization and a modified OAM given by $m'\hbar$ (plus a uniform phase shift of $\pm 2\alpha_0$). The relative amplitude of these two components of the output field is fixed by the birefringent retardation δ.

A q-plate is said to be *tuned* if $\delta = \pi$ (modulo 2π), so as to cancel the first wave, i.e. that having unchanged properties, and hence to obtain a maximal (in principle unitary) conversion of the input wave into the second term, i.e. the wave having reshaped wavefront. A precise tuning of the q-plate can be obtained by acting on the LC cell via a suitable external control-parameter, such as the cell temperature or an applied voltage. In particular, a temperature control can be used for adjusting the LC birefringence Δn [15]. A static or low-frequency electric field can be used instead for reorienting the LC director in a tilted orientation with respect to the *xy* plane, so as to decrease its effective birefringence, while keeping the same projected director pattern on the *xy* plane, as specified by Eq. (1) [17].

It can be useful to introduce a quantum notation to describe the optical effect of a q-plate. For the case of a tuned q-plate, the transformations induced by the q-plate on circularly polarized light carrying OAM can be then rewritten as follows:

$$\begin{aligned} |L,m\rangle &\xrightarrow{\text{q-plate}} |R,m+2q\rangle \\ |R,m\rangle &\xrightarrow{\text{q-plate}} |L,m-2q\rangle \end{aligned} \tag{6}$$

where the first symbol in the ket indicates the polarization state (L, for left-circular and R for right-circular) and the second is the OAM quantum number. This behavior is pictorially illustrated in Fig. 1. Most importantly, the q-plate is a coherent device that conserves linear combinations, so that an input light having an arbitrary (generally elliptical) polarization is transformed according to the following law:

$$(\alpha|L\rangle_\pi + \beta|R\rangle_\pi)|m\rangle_o = \alpha|L,m\rangle + \beta|R,m\rangle \xrightarrow{\text{q-plate}} \alpha|R,m+2q\rangle + \beta|L,m-2q\rangle. \tag{7}$$

In the first expression on the left-hand-side of this equation we have used a notation separating the polarization degree of freedom (labeled with a subscript π) and the OAM one (labeled with a subscript o), so as to show more clearly that the input wave has a single well-defined elliptical polarization and a single OAM value. At the output, on the contrary, we obtain a non-separable optical state, in which polarization and OAM are "entangled" (although there is no non-locality involved in this form of entanglement). For a classical wave, this non-separability corresponds simply to the fact that the polarization is not uniform across the wave cross-section. An example of such output field is shown in Fig. 2.

We should emphasize that Eqs. (6) and (7) omit to describe the effect of the q-plate on the radial profile of the optical wave. This effect has been discussed in Refs. [20–22]. In many applications, this radial effect can be ignored, either because the radial profile

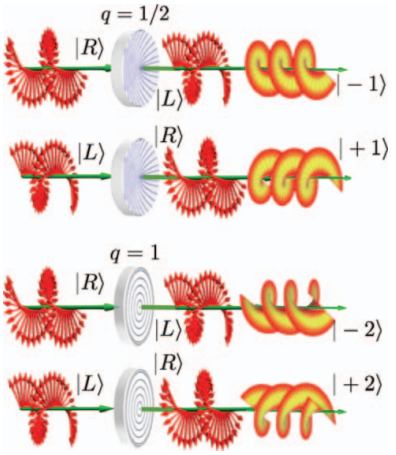

Figure 1. Effect of a tuned q-plate on input circularly polarized light having zero OAM. The upper two panels illustrate the case $q = \frac{1}{2}$ for the two opposite circular polarizations. The lower two panels refer to the case $q = 1$. In all cases, the output polarization handedness is inverted and the output OAM acquires $\pm 2q\hbar$ of angular momentum, with the $\pm$ sign determined by the input polarization handedness [11].

factorizes and therefore is the same for all field components or because the propagation occurs on a sufficiently short distance that its effects remain negligible. Conversely, in some other cases, the working principle of the desired application depends on the radial effects arising from the q-plate and on the subsequent free optical propagation [15–16].

The first q-plates were prepared by a circular rubbing procedure [12], which was well suited only for the pattern with $q = 1$. More recently, we have moved on to a non-contact photo-alignment technique, allowing for a preparation of electrically-tuned q-plates with

Figure 2. Calculated pattern of intensity (in false colors) and polarization (arrows) for the optical field that emerges from a tuned q-plate with $q = 1$ when the input light is linearly polarized (with horizontal orientation, relative to the figure). It can be seen that the output intensity is shaped as a doughnut and the polarization is everywhere linear but space-variant, so that polarization and transverse mode result to be non-separable properties. In the quantum language, the spin and the OAM of a single photon are entangled [28, 29].

arbitrary topological charge q [18]. A similar technique has been also used by other groups for preparing polymer-LC q-plates, although these devices do not include the electric tuning feature [19].

III. A Physical Mapping Between Polarization and OAM

Since its first introduction, in 2006, the q-plate has found already a number of applications. Many of them share a common underlying concept, i.e. the use of the q-plate for creating a *physical mapping between polarization and a two-dimensional (2D) subspace of OAM*. The mapping allows for the control of output OAM (within the subspace) using the input polarization of light, or vice versa. This in turn can be used for transferring the information (quantum or classical) contained in one property of the light into the other property. These transfer devices have been used to demonstrate many interesting quantum information processes, as will be reviewed in the next Section. Here, we focus instead on how the q-plate can be used to give rise to this physical mapping between polarization and OAM.

The concept of this mapping is pictorially illustrated in Fig. 3. The 2D space of polarization is represented by the Poincaré sphere (corresponding to Bloch's sphere for generic 2D quantum spaces). A similar Poincaré-like representation can be used for any 2D subspace of OAM [23]. In particular, we are interested here in the OAM subspaces generated by a pair of opposite m modes ($|m\rangle$, $|-m\rangle$), which will be denoted as $o_{|m|}$. A q-plate in combination with other optical elements can be used to implement this mapping very simply, that is to convert an input mode that is described by a given point on one of the two spheres into the corresponding point on the other sphere, or vice versa. There exist both unitary and non-unitary optical schemes to accomplish this task. The non-unitary schemes waste a fraction of the input optical energy (i.e., they are 'probabilistic', in the language of quantum information, because a fraction of the photons are lost). However they can also be very simple. For example, a single q-plate followed by a linear polarizer can be used to

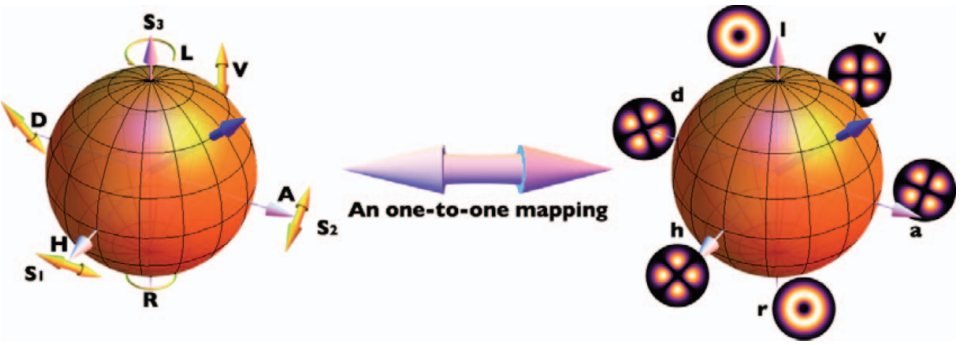

Figure 3. Sketch of the Poincaré sphere representing the space of all possible polarizations (left) and the Poincaré-like sphere representing a 2D subspace of OAM (right) [23]. The double arrow connecting the two symbolizes the one-to-one mapping that can be created using the q-plate in combination with other devices. The Poincaré sphere orientation is here chosen so as to have the circular polarizations (L = left and R = right) at the poles and the linear polarizations on the equator (in particular, H = horizontal, V = vertical, D = diagonal, A = anti-diagonal), while the OAM Poincaré-like sphere has the OAM eigenmodes (l and r) at the poles and the Hermite-Gauss-like modes on the equator (in particular, h, v, d, a). The intensity patterns of some OAM modes is also sketched close to the sphere, for the case of an OAM with $|m| = 2$.

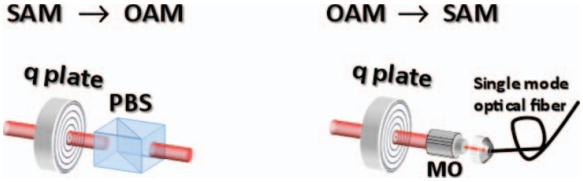

Figure 4. Pictorial representation of the simplest non-unitary (probabilistic) devices for the transfer of a qubit of quantum information from the polarization to the OAM (SAM → OAM) and vice versa (OAM → SAM) [22, 29]. The first is based on a q-plate and a polarizing beam splitter (PBS). The second requires a q-plate and a zero-OAM-filter, as obtained by coupling into a single mode fiber (using a microscope objective, MO).

transfer the polarization input state into the corresponding OAM subspace o_l with $l = 2|q|$ (irrespective of the value of α_0, which affects only a global phase), while a q-plate followed by an OAM $m = 0$ filter (such as an iris, or a single-mode fiber) can be used to transfer the OAM input mode into the polarization one [22]. These schemes, illustrated in Fig. 4, have a 50% efficiency (or success probability), i.e. half of the input energy (or photon number) is lost in the conversion.

A 100% efficient unitary mapping, allowing for reversible mode conversion, can be obtained by combining a q-plate with an interferometer containing one or two Dove prisms [22, 24]. The most convenient geometry choice for the interferometer is the Sagnac one, which ensures a high stability and has been generally shown to be a very convenient tool for OAM manipulations [25]. This scheme, illustrated in Fig. 5, is fully reciprocal and can therefore work in both directions.

This scheme was demonstrated experimentally in the classical regime [24] and very recently in the quantum single photon one [26]. Examples of the resulting modes on the OAM-Poincaré sphere for $|m| = 2$ and continuous variations of the input polarization are given in Fig. 6. The interference fringes with a plane reference wave, also shown in the figure, were used to analyze the output mode phase structure.

We stress that this setup can generate a class of azimuthal transverse modes belonging to the given OAM subspace, including all modes that have the same azimuthal structure as the Hermite–Gaussian modes, with a theoretical efficiency of 100%. The choice of the

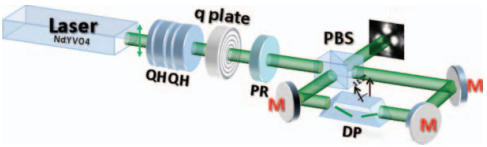

Figure 5. Sketch of the experimental setup that can be used for creating a unitary (deterministic) mapping of the polarization space and an OAM subspace (adapted from [24]). The layout shown is that used to convert the polarization state into an OAM mode, but the converse is obtained by reversing the propagation direction of light (i.e., swapping the input and output lines). The QHQH set is a sequence of wave-plates used to select any given input polarization starting from the laser linear polarization, so it is not part of the "mapping" setup. The latter is instead composed of the q-plate, a polarization rotator (PR) and the Sagnac interferometer comprising three mirrors (M), a polarizing beam-splitter (PBS), and a Dove prism (DP) rotated at an angle of 11.25°.

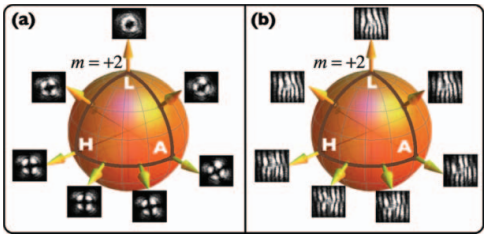

Figure 6. Sequence of transverse modes belonging to an OAM bidimensional subspace with $|m| = 2$ obtained using the mapping setup shown in Fig. 5 and varying the input polarization. The OAM modes are shown in correspondence with the relative points on the Poincaré-like sphere. Both intensity patterns (a) and interference fringes with a plane reference used to determine the phase pattern (b) are shown (adapted from [24]).

generated mode is entirely controlled by the input polarization, which can be manipulated at very fast rates, in contrast to what can be obtained with a spatial light modulator.

IV. Survey of q-Plate Quantum Applications

The optical OAM has started being considered as a possible useful resource for photonic quantum information science and technology since 2001, after Zeilinger's group demonstrated generation of OAM-entangled photons by spontaneous parametric down conversion (SPDC) [27]. That the q-plate device could find particularly interesting applications in the quantum information field was immediately noticed and proposed theoretically [11, 28], but the first experimental demonstration of the use of q-plates in the single-photon quantum regime had to wait a few years [29]. The surprisingly good resilience to optical misalignments of the OAM-encoded qubits prepared and analyzed using q-plates or other mode perturbations has been recently investigated [30].

Most of the applications of the q-plate demonstrated so far descend from the mapping devices discussed in the previous section. In particular, in the quantum domain, these devices allow one to obtain a transfer of quantum information from the polarization (or SAM) subspace to the OAM one and vice versa. For example a single qubit initially encoded in the polarization of a single photon can be transferred to the OAM or vice versa by a transfer device, as was demonstrated first with probabilistic (non-unitary) schemes [22, 29] and very recently also with a deterministic setup [26].

The ability to transfer the qubit state allows for the standard methods of polarization-encoded quantum information to be applied also to OAM-encoded qubits. This has for example led to the first experimental demonstration of the Hong-Ou-Mandel effect performed with OAM-carrying single photons, and to the associated first experimental implementation of the optimal quantum cloning protocol [31]. Another application of the qubit transfer devices was for demonstrating hybrid-entangled pairs of photons, i.e. an entanglement in which the polarization state of one photon is entangled with the OAM state of the other photon. This was obtained by two alternative methods: (i) generating polarization-entangled pairs (by type-II SPDC) and subsequently converting the polarization state of one of the photons into OAM [32]; (ii) generating OAM-entangled pairs (by type-I SPDC) and then converting the OAM state of one of the photons into polarization [33]. The generated hybrid photon pairs were also used to explore the issues of quantum non-locality and quantum non-contextuality from a new perspective [33].

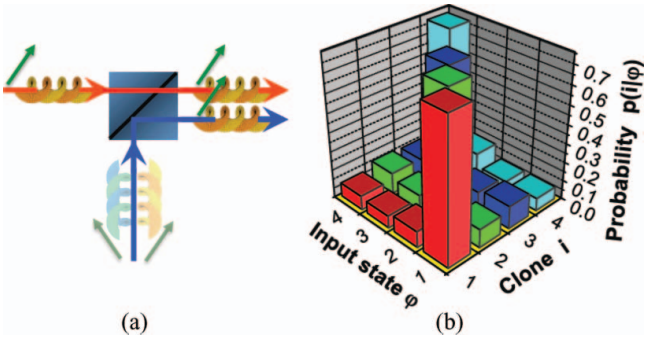

Figure 7. Optimal quantum cloning of photonic ququarts obtained by combining polarization and OAM of single photons (Refs. [34, 35]). Panel (a) gives a pictorial representation of the cloning process based on the symmetrization method. This requires using a balanced beam splitter. The photon to be cloned must enter the beam splitter from one input port, while a photon in a fully randomized state (within the working Hilbert space) must enter the other input port. The cloning succeeds if the two photons emerge from the same output port of the beam splitter. In this case, the copying fidelity is maximal, i.e. equal to 0.7 (this limit applies to quantum space dimension $d = 4$). Panel (b) shows the experimental copying probabilities for each given input state chosen among four basis states and the corresponding four outputs [35]. It can be seen that exact copies are obtained with a probability of about 0.7, as predicted theoretically, while inexact copies have a probability of 0.1 for each state of the basis.

The main potential advantage of using OAM for quantum information is that of using its higher dimensionality or its combination with polarization for encoding more qubits in a single photon, or equivalently to encode in each photon a so-called "qudit", i.e., a quantum state living in a d-dimensional space with $d > 2$, in each photon.

We have recently started to exploit this possibility by demonstrating for the first time the generation and measurement of photonic ququarts (i.e., qudits with $d = 4$) based on both polarization and OAM, by exploiting q-plate-based schemes [34]. Next, we have demonstrated the first quantum protocol with these photon ququarts, i.e. optimal quantum cloning, which is pictorially illustrated in Fig. 7 [35]. These steps provide a first proof-of-principle demonstration of the potential of OAM for higher-dimensional quantum information technology.

In conclusion, in the last few years a number of advances in the field of OAM sprung from the introduction of the liquid crystal q-plate. This device, by allowing for a strong effective coupling of the spin and OAM of a photon, has shown a great potential for developing new classical and quantum photonic applications, and there are good reasons to expect that many others will follow.

We acknowledge the financial support of the Future and Emerging Technologies (FET) programme within the Seventh Framework Programme for Research of the European Commission, under FET-Open grant number 255914, PHORBITECH.

References

[1] Molina-Terriza, G., Torres, J. P., & Torner, L. (2007). *Nature Phys. 3*, 305.
[2] Franke-Arnold, S., Allen, L., & Padgett, M. J. (2008). *Laser & Photon. Rev.*, *2*, 299.
[3] Blinov, L. M., & Chigrinov, V. G. (1996). *Electrooptic Effects in Liquid Crystal Materials*, Springer, New York.

[4] Santamato, E., Maddalena, P., Marrucci, L., & Piccirillo, B. (1998). *Liq. Cryst.*, *25*, 357.
[5] Santamato, E. *et al.* (1999). *Mol. Cryst. Liq. Cryst. 328*, 479.
[6] Marrucci, L. *et al.* (1998). *Phys. Rev. A 58*, 4926.
[7] Kreuzer, M., Marrucci, L., & Paparo, D. (2000). *J. Nonlinear Opt. Phys. Mater.*, *9*, 157.
[8] Kreuzer, M. *et al.* (2002). *Phys. Rev. Lett.*, *88*, 013902.
[9] Kreuzer, M. *et al.* (2003). *Phys. Rev. E*, *68*, 011701.
[10] Manzo, C., Paparo, D., Marrucci, L., & Jánossy, I. (2006). *Phys. Rev. E*, *73*, 051707.
[11] Marrucci, L., Manzo, C., & Paparo, D. (2006). *Phys. Rev. Lett.*, *96*, 163905.
[12] Marrucci, L., Manzo, C., & Paparo, D. (2006). *Appl. Phys. Lett.*, *88*, 221102.
[13] Marrucci, L. (2008). *Mol. Cryst. Liq. Cryst.*, *488*, 148.
[14] Marrucci, L. *et al.* (2011). *J. Opt.*, *13*, 064001.
[15] Karimi, E. *et al.* (2009). *Appl. Phys. Lett.*, *94*, 231124.
[16] Slussarenko, S. *et al.* (2009). *Phys. Rev. A*, *80*, 022326.
[17] Piccirillo, B. *et al.* (2010). *Appl. Phys. Lett.*, *97*, 241104.
[18] Slussarenko, S. *et al.* (2011). *Opt. Express 19*, 4085.
[19] Nersisyan, S., Tabiryan, N., Steeves, D. M., & Kimball, B. R. (2009). *Opt. Express 17*, 11926.
[20] Karimi, E. *et al.* (2007). *Opt. Lett.*, *32*, 3053.
[21] Karimi, E., Piccirillo, B., Marrucci, L., & Santamato, E. (2009). *Opt. Lett.*, *34*, 1225.
[22] Nagali, E. *et al.* (2009). *Opt. Express*, *17*, 18745.
[23] Padgett, M. J., Courtial, J. (1999). *Opt. Lett.*, *24*, 430.
[24] Karimi, E. *et al.* (2010). *Phys. Rev. A*, *81*, 053813.
[25] Slussarenko, S. *et al.* (2010). *Opt. Express*, *18*, 27205–27216.
[26] D'Ambrosio, V. *et al.* (2012). *Opt. Lett.*, *37*, 172.
[27] Mair, A., Vaziri, A., Weihs, G., & Zeilinger, A. (2001). *Nature 412*, 313.
[28] Marrucci, L. (2007). *Proceedings of SPIE 6587*, 658708.
[29] Nagali, E. *et al.* (2009). *Phys. Rev. Lett.*, *103*, 013601.
[30] Giovannini, D., Nagali, E., Marrucci, L., & Sciarrino, F. (2011). *Phys. Rev. A*, *83*, 042338.
[31] Nagali, E. *et al.* (2009). *Nature Photon.*, *3*, 720–723.
[32] Nagali, E., & Sciarrino, F. (2010). *Opt. Express*, *18*, 18243.
[33] Karimi, E. *et al.* (2010). *Phys. Rev. A*, *82*, 022115.
[34] Nagali, E. *et al.* (2010). *Phys. Rev. A*, *81*, 052317.
[35] Nagali, E. *et al.* (2010). *Phys. Rev. Lett.*, *105*, 073602.